



# A New Perspective on Li-SO<sub>2</sub> Batteries for Rechargeable Systems\*\*

Hee-Dae Lim, Hyeokjun Park, Hyungsub Kim, Jinsoo Kim, Byungju Lee, Youngjoon Bae, Hyeokjo Gwon, and Kisuk Kang\*

**Abstract:** Primary Li-SO<sub>2</sub> batteries offer a high energy density in a wide operating temperature range with exceptionally long shelf life and have thus been frequently used in military and aerospace applications. Although these batteries have never been demonstrated as a rechargeable system, herein, we show that the reversible formation of Li<sub>2</sub>S<sub>2</sub>O<sub>4</sub>, the major discharge product of Li-SO<sub>2</sub> battery, is possible with a remarkably smaller charging polarization than that of a Li-O<sub>2</sub> battery without the use of catalysts. The rechargeable Li-SO<sub>2</sub> battery can deliver approximately 5400 mAh g<sup>-1</sup> at 3.1 V, which is slightly higher than the performance of a Li-O<sub>2</sub> battery. In addition, the Li-SO<sub>2</sub> battery can be operated with the aid of a redox mediator, exhibiting an overall polarization of less than 0.3 V, which results in one of the highest energy efficiencies achieved for Li-gas battery systems.

Revisiting conventional primary batteries sometimes inspires new chemistry that can be adopted in rechargeable batteries. The recent rapid growth of the Li-O<sub>2</sub> battery field is an example of the successful evolution from a primary battery to a secondary battery.<sup>[1,2]</sup> Although it was previously conceived that a metal-O<sub>2</sub> system was only suitable for primary batteries, the current Li-O<sub>2</sub> system has become one of the most promising candidates for next-generation secondary batteries, specifically considering that it can deliver an exceptionally high energy density at a level unattainable by conventional lithium-ion batteries.<sup>[3-5]</sup> Exploring a new chemistry in metal-gas systems plays a key role in the development of ultra-high energy density batteries, as it enables electrochemical energy storage without the use of a heavy transition-metal redox host. Recent reports on various metal-gas rechargeable batteries, such as Na-O<sub>2</sub>, K-O<sub>2</sub>, Al-O<sub>2</sub>, and Li-CO<sub>2</sub> systems, reveal their potential applicability as high-energy-storage media with unique elec-

trochemical properties depending on the combination of metal and gas.<sup>[6-12]</sup>

The concept of a primary Li-SO<sub>2</sub> cell was first reported in the late 1960s.<sup>[13,14]</sup> It operates based on the reaction between lithium ions and sulfur dioxide, which produces Li<sub>2</sub>S<sub>2</sub>O<sub>4</sub> (lithium dithionite) as a discharge product, delivering an energy density of about 330 Wh kg<sup>-1</sup>.<sup>[15-17]</sup> The sulfur dioxide is initially dissolved or liquefied in the electrolyte of a sealed cell with lithium metal as the anode and porous carbon as the cathode. Earlier Li-SO<sub>2</sub> systems needed to use a pressurized cell; however, recent works have successfully demonstrated that an ambient pressure cell is also achievable with the proper selection of an electrolyte that can dissolve a sufficiently large amount of sulfur dioxide.<sup>[16]</sup> Although the Li-SO<sub>2</sub> cell has never been demonstrated in rechargeable conditions with a gas inlet and outlet, the chemistry resembles that of the Li-O<sub>2</sub> system in many ways. During discharging, the gas phase receives electrons from the electrode surface, which subsequently combine with lithium ions to finally form lithium-containing solid discharge products. The porous electrode accommodates a large amount of solid products to achieve a high capacity and gradually fill the pores, which results in an increase in the impedance of the cell and finally the end of the discharge. Herein, we demonstrate that the charging reaction is also feasible in Li-SO<sub>2</sub> batteries, similar to Li-O<sub>2</sub>, which can be reversibly operated using an organic electrolyte through the formation/decomposition of Li<sub>2</sub>S<sub>2</sub>O<sub>4</sub>. The initial discharge capacity is as high as that of Li-O<sub>2</sub> batteries (ca. 5400 mAh g<sup>-1</sup>); however, the energy efficiency is significantly better without the use of catalysts. The working mechanism of rechargeable Li-SO<sub>2</sub> batteries can guide the development of a new metal-gas system and also aid in our understanding of the current limitation of the Li-O<sub>2</sub> system.

The working principle of a rechargeable Li-SO<sub>2</sub> battery is described in Figure 1 a. Unlike the primary battery setup, the cell design consists of an electrode that is open to a SO<sub>2</sub> atmosphere using a Swagelok-type cell. During the discharge process, the porous carbon cathode enables an influx of SO<sub>2</sub> gas and provides reaction sites for the lithium ions and SO<sub>2</sub> to accommodate the discharge product, Li<sub>2</sub>S<sub>2</sub>O<sub>4</sub>. During the charging process, the discharge products are expected to be decomposed and evolve SO<sub>2</sub> gas from the electrode. Figure 1 b shows a typical discharge/charge profile of the Li-SO<sub>2</sub> battery along with that of the reference Li-O<sub>2</sub> battery under the same operation conditions. The discharge potential and profile are in a good agreement with those of the primary cell, indicating that the SO<sub>2</sub> reacted electrochemically with Li ions.<sup>[18,19]</sup> It is notable that the charging process is possible with overall electrochemical profiles similar to those of Li-O<sub>2</sub> cells. We observed that the charging process results in a significant amount of sulfur dioxide gas evolution, as

[\*] H.-D. Lim,<sup>[†]</sup> H. Park,<sup>[†]</sup> H. Kim, J. Kim, B. Lee, Y. Bae, Prof. K. Kang  
Department of Materials Science and Engineering  
Seoul National University  
Seoul 151-742 (Republic of Korea)  
E-mail: matlgen1@snu.ac.kr

H. Gwon  
Department of Materials Science and Engineering, KAIST  
Daejeon 305-701 (Republic of Korea)

[†] These authors contributed equally to this work.

[\*\*] This work was supported by a National Research Foundation of Korea Grant funded by the Korean Government (MEST) (NRF-2009-0094219), and by the Human Resources Development program (20124010203320) of the Korea Institute of Energy Technology Evaluation and Planning (KETEP) grant funded by the Korea government Ministry of Trade, Industry and Energy.

Supporting information for this article is available on the WWW under <http://dx.doi.org/10.1002/anie.201504306>.

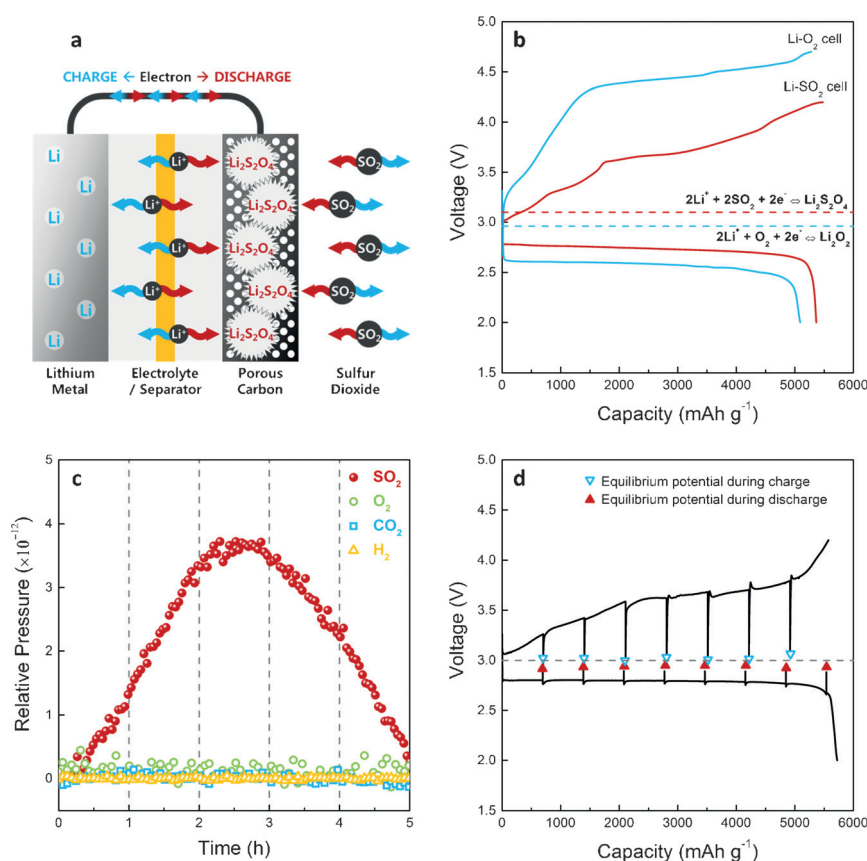


**Figure 1.** a) Schematic illustration of the concept of a rechargeable Li-SO<sub>2</sub> battery during discharge and charge. b) Comparison of the electrochemical profiles of Li-O<sub>2</sub> and Li-SO<sub>2</sub> batteries at a current density of 0.2 mA cm<sup>-2</sup>. The theoretical formation potentials of Li<sub>2</sub>O<sub>2</sub> and Li<sub>2</sub>S<sub>2</sub>O<sub>4</sub> are 2.96 and 3.1 V vs. Li/Li<sup>+</sup>, respectively. c) Gas evolution profile during charge process of Li-SO<sub>2</sub> cell with limited capacity of 1 mAh obtained using in situ DEMS analysis. d) Galvanostatic intermittent titration technique (GITT) voltage profile of Li-SO<sub>2</sub> cell. The discharge capacities were calculated based on the cathode carbon weight.

demonstrated in Figure 1c. The in situ differential electrochemical mass spectrometry (DEMS) experiment in Figure 1c detected the evolution of sulfur dioxide throughout the charging process without other gases such as carbon dioxide, oxygen, or hydrogen. The absence of other gases implies

of the cathode in the Li-SO<sub>2</sub> battery at a few stages of discharge and charge. At each step, the cathode was carefully washed using the TEGDME solvent and dried before the test. All the procedures were performed in a glove box without air exposure. The results clearly demonstrate that the gradual

a stable charging reaction in the cell, in contrast to conventional Li-O<sub>2</sub> cells, which exhibit a detectable level of carbon monoxide or dioxide evolution resulting from the partial corrosion of the carbon electrode or decomposition of the electrolyte.<sup>[20]</sup> The discharge capacity is comparable to that of a Li-O<sub>2</sub> cell; however, the voltage of the Li-SO<sub>2</sub> cell is higher by approximately 300 mV because the formation of the Li<sub>2</sub>S<sub>2</sub>O<sub>4</sub> discharge product yields a greater Gibbs free energy change in the reaction.<sup>[21]</sup> The charging polarization of the Li-SO<sub>2</sub> cell is markedly lower than that of the Li-O<sub>2</sub> cell even without a catalyst. The completion of the charging process could be done below 4 V. Consequently, the observed energy efficiency of the Li-SO<sub>2</sub> system is significantly higher than that of the Li-O<sub>2</sub> system. In Figure 1d, we used the galvanostatic intermittent titration technique (GITT) to determine the thermodynamic potential of the reaction. After full relaxations, the quasi-open circuit potential of each step is close to the theoretical voltage of Li<sub>2</sub>S<sub>2</sub>O<sub>4</sub> formation, which also supports the conclusion that the discharge/charge reaction mainly involves the formation/decomposition of Li<sub>2</sub>S<sub>2</sub>O<sub>4</sub>.

Using ex situ analyses, we attempted to verify that the charging process was the result of the electrochemical decomposition of Li<sub>2</sub>S<sub>2</sub>O<sub>4</sub>. Figure 2 presents ex situ X-ray diffraction (XRD) patterns

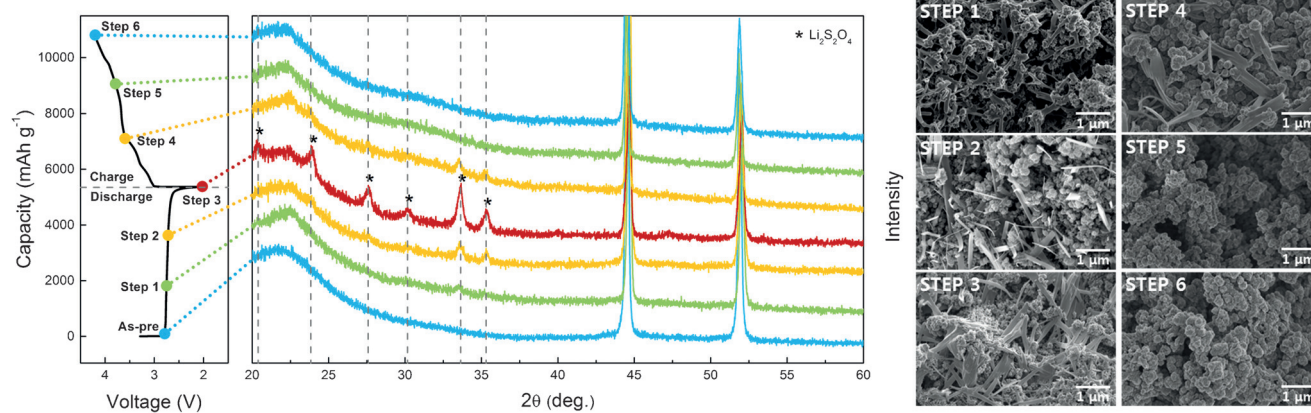


**Figure 2.** Ex situ XRD and SEM analysis of a Li-SO<sub>2</sub> battery at each step. The dotted lines correspond to Li<sub>2</sub>S<sub>2</sub>O<sub>4</sub>, and the high intensity peaks near 44° and 52° correspond to the Ni mesh current collector. All figures were viewed under the same magnification.

formation and decomposition of  $\text{Li}_2\text{S}_2\text{O}_4$  occur on the cathode. Upon discharge to step 1, the XRD peaks begin to evolve at  $33.5^\circ$  and  $35.4^\circ$ , which correspond to the characteristic peaks observed for  $\text{Li}_2\text{S}_2\text{O}_4$ .<sup>[22]</sup> After further discharge, the peaks grow substantially with additional peaks appearing at  $27.5^\circ$  and  $30.1^\circ$ . However, the intensities of these peaks decrease during charging and completely disappear at the end of the charge, suggesting that the decomposition of  $\text{Li}_2\text{S}_2\text{O}_4$  primarily occurs during charging. The relatively sharp peaks of  $\text{Li}_2\text{S}_2\text{O}_4$  appearing during a cycle are slightly different from those of the  $\text{Li}-\text{O}_2$  cell, where the XRD signature of lithium peroxide ( $\text{Li}_2\text{O}_2$ ) is sometimes difficult to detect.<sup>[23–26]</sup> This result hints at the relatively high crystallinity of the discharge product for the  $\text{Li}-\text{SO}_2$  battery.

Consistent with the XRD results, the crystalline size of the discharge products was large after discharge, as observed in the SEM images in Figure 2. In the porous carbon electrode, the  $\text{Li}_2\text{S}_2\text{O}_4$  gradually grows into a nanoribbon-like morphology from discharge steps 1 to 3. The nanoribbon shape of the discharge product with a length of a few micrometers and a width of hundreds of nanometers differs from the toroid or film-like morphology of  $\text{Li}_2\text{O}_2$ <sup>[27,28]</sup> in  $\text{Li}-\text{O}_2$  cells or the cubic shape of  $\text{NaO}_2$ <sup>[8,29]</sup> in  $\text{Na}-\text{O}_2$  cells. Because the morphology of the discharge products is closely related to the reaction mechanism involving the soluble intermediate discharge phase, a more detailed study will be required on this phenomenon.<sup>[30,31]</sup> Upon full discharge to 2.0 V, the nanoribbon fills up nearly all of the void spaces of the carbon electrode (step 3). During the charging process, the discharge product gradually disappears; after step 5 (charge to ca. 3.8 V), most of the ribbon-like discharge products cannot be observed, and the pristine state of the carbon electrode is recovered. Additional SEM images of the cathode at lower magnification are presented in Figure S1 in the Supporting Information.

The use of catalysts could further enhance the efficiency of the  $\text{Li}-\text{SO}_2$  cell by further reducing the charging polarization. As a model catalyst, a lithium iodide ( $\text{LiI}$ ) soluble catalyst was adopted in the system, which was recently demonstrated to be an efficient redox mediator in the decomposition of  $\text{Li}_2\text{O}_2$  in  $\text{Li}-\text{O}_2$  batteries.<sup>[4,11,32]</sup> Figure 3a compares the electrochemical profiles of  $\text{Li}-\text{SO}_2$  cells with (blue) and without (red) the catalyst. The addition of the catalyst led to a clear and significant decrease of the polarization during the charging process. The overall charge polarization was reduced to less than 0.3 V, which leads to a significant enhancement of the energy efficiency. Note that

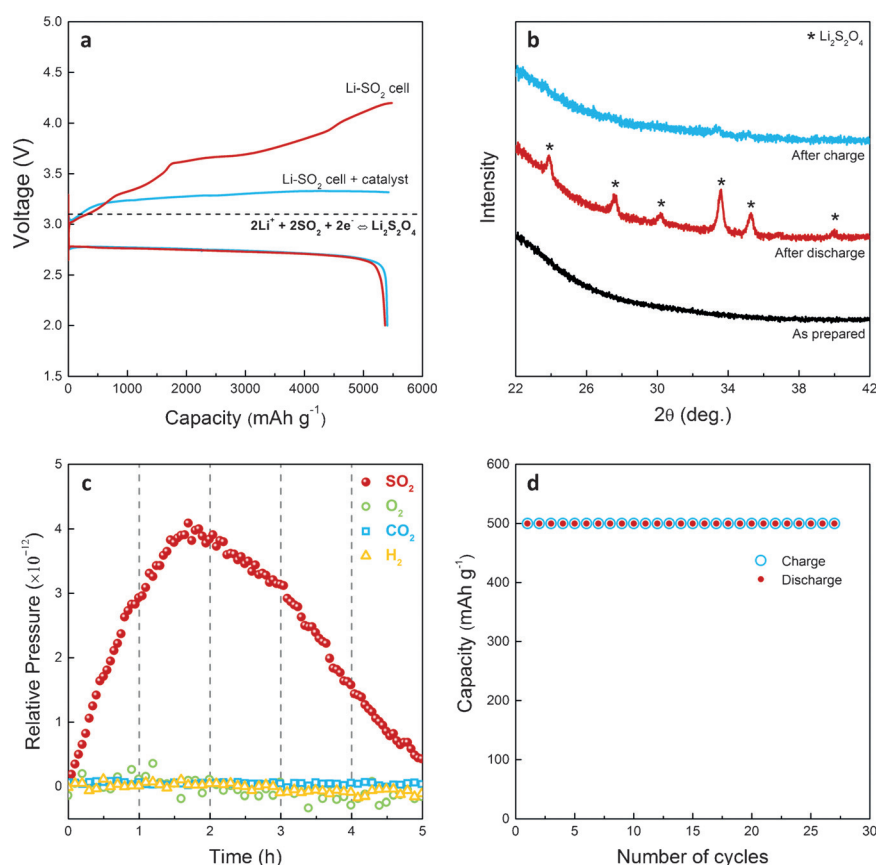


**Figure 3.** a) Comparison of the electrochemical profiles of the  $\text{Li}-\text{SO}_2$  cell without and with a catalyst. b) XRD results of the  $\text{Li}-\text{SO}_2$  cell using a catalyst. c) In situ DEMS result; gas evolution as a function of time during the charge process of the  $\text{Li}-\text{SO}_2$  cell with  $\text{LiI}$  catalyst. d) Cyclability of the  $\text{Li}-\text{SO}_2$  cell with the catalyst utilized up to  $500 \text{ mAh g}^{-1}$ .

the oxidized form of  $\text{LiI}$  ( $\text{I}_2$  or  $\text{I}_3^-$ ) effectively decomposes  $\text{Li}_2\text{S}_2\text{O}_4$  via a chemical reaction, similar to the reaction with  $\text{Li}_2\text{O}_2$ ; however, it is more effective in the  $\text{Li}-\text{SO}_2$  system because the equilibrium potential of  $\text{Li}_2\text{S}_2\text{O}_4$  formation (ca. 3.1 V) is closer to the redox potential of  $\text{I}^-/\text{I}_3^-$  (or  $\text{I}^-/\text{I}_2$ ) (ca. 3.4 V) than that of  $\text{Li}_2\text{O}_2$  formation (ca. 2.96 V). Therefore, the theoretical charging efficiency using  $\text{LiI}$  in  $\text{Li}-\text{SO}_2$  batteries can be as high as 91%, which is substantially higher than that in  $\text{Li}-\text{O}_2$  batteries. The ex situ XRD analysis (Figure 3b) demonstrates the reversible formation and decomposition of  $\text{Li}_2\text{S}_2\text{O}_4$  within a much narrower voltage range (2.0–3.2 V) using the catalyst, which indicates that  $\text{LiI}$  could effectively decompose the discharge product. The catalytic activity of  $\text{LiI}$  in  $\text{Li}-\text{SO}_2$  cells was also confirmed by in situ DEMS analysis. The DEMS result in Figure 3c shows that sulfur dioxide ( $\text{SO}_2$ ) was solely evolved during the charging process without any other gas evolution. Cycling of the cell using  $\text{LiI}$  was thus possible, and under a capacity-limited condition of  $500 \text{ mAh g}^{-1}$ , the cycling continued for more than 25 cycles, as demonstrated in Figure 3d.

The capacity retention was not remarkable at this stage, even though  $\text{Li}_2\text{S}_2\text{O}_4$  could be electrochemically decomposed as demonstrated above. Less than  $1000 \text{ mAh g}^{-1}$  could be retained after ten cycles when operated without catalysts between 2.0–4.2 V, as shown in the Figure S2. This perfor-



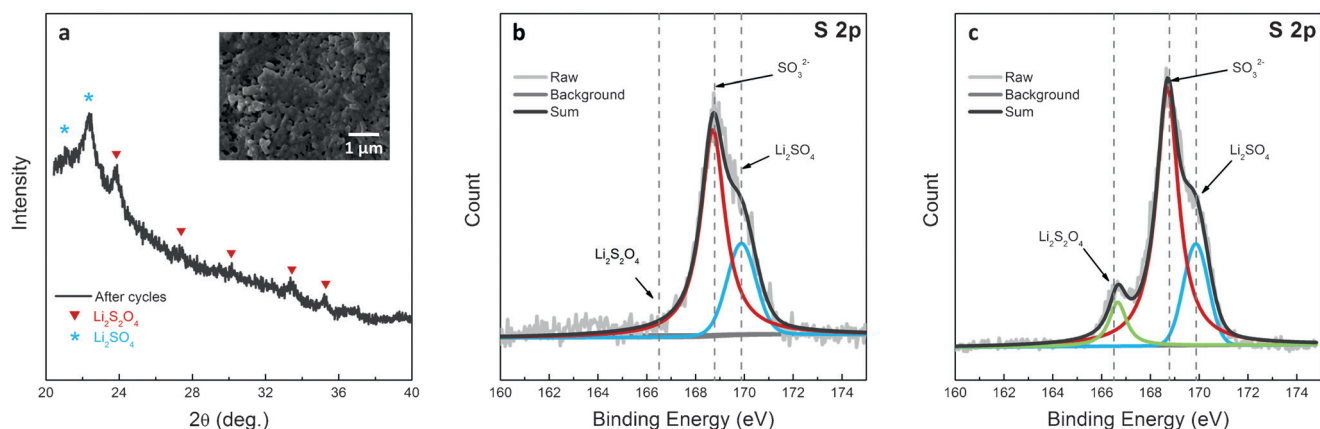


**Figure 4.** a) XRD pattern of the cathode after cycling (inset: SEM image of the cathode after cycling). XPS spectra of S 2p: b) after re-charge and c) at the end of cycling. The overall peaks are arranged based on the reference C–C bond at 284.5 eV.

mance level is only comparable to that of early Li–O<sub>2</sub> batteries.<sup>[33,34]</sup> To investigate the origin of the cycle degradation, we examined the cathode after the end of the cycling process using XRD, and the results are presented in Figure 4a. In addition to the main discharge product, Li<sub>2</sub>S<sub>2</sub>O<sub>4</sub>, a trace of the Li<sub>2</sub>SO<sub>4</sub> phase could also be detected, which was observed to cover the surface of the cathode by SEM (inset of Figure 4a). It implies that the rapid deterioration of the cell is most likely due to the residual byproducts on the surface of the cathode. For a closer investigation of the formation of byproducts on the surface, the surface was characterized by X-ray photoelectron spectroscopy (XPS), as shown in Figure 4b and c. After the first discharge, two major peaks dominated, corresponding to Li<sub>2</sub>S<sub>2</sub>O<sub>4</sub> and Li<sub>2</sub>SO<sub>3</sub> in the Figure S3 (XPS spectra of S 2p) with a trace of Li<sub>2</sub>SO<sub>4</sub>.<sup>[16]</sup> Although the peak of Li<sub>2</sub>S<sub>2</sub>O<sub>4</sub> disappears after charging, which again indicates the reversible decomposition of Li<sub>2</sub>S<sub>2</sub>O<sub>4</sub> during the charging process, the peaks from Li<sub>2</sub>SO<sub>3</sub> and Li<sub>2</sub>SO<sub>4</sub> do not completely disappear (Figure 4b). At the end of the cycling, residual amounts of Li<sub>2</sub>SO<sub>3</sub> are still detected along with the unreacted Li<sub>2</sub>S<sub>2</sub>O<sub>4</sub>. It is presumed that the byproducts remaining after charging are gradually deposited onto the carbon surface during cycling. This passivation layer may block the active pores while also contributing to the decrease in the electrical conductivity of the cathode. Suppression or elimination of the byproducts will be key to further enhancing the cyclability.

Another practical barrier for the realization of a rechargeable Li–SO<sub>2</sub> battery is the use of sulfur dioxide gas. Although sulfur dioxide is naturally released by volcanic activity and is widely used in winemaking as a preservative,<sup>[35]</sup> it is inherently a harmful gas. The emission of the gas into the atmosphere will not be desirable when charging the battery. As an alternative, in this respect, the rechargeable Li–SO<sub>2</sub> battery can be designed with a closed-cell type, where the circulation of the gas is confined within the cell. An interesting characteristic of SO<sub>2</sub> gas is that a substantially large amount of gas can be dissolved in the organic solvent, representing one of the highest solubilities among gases.<sup>[36]</sup> In addition, with slight pressurization, the soluble amount can be significantly increased, which explains why pressurized Li–SO<sub>2</sub> was

one of the first systems to be commercialized in metal-gas batteries. Even without pressurization, it is noteworthy that the recent finding on ionic liquids as an electrolyte in primary Li–SO<sub>2</sub> could achieve a large amount of SO<sub>2</sub> gas dissolution at ambient pressure, resulting in a high energy density.<sup>[16]</sup> This finding implies that closed-type rechargeable Li–SO<sub>2</sub> batteries without the emission of harmful gases are feasible and that consideration of a smart cell design can make use of the high-energy rechargeable Li–SO<sub>2</sub> chemistry.

In summary, a rechargeable Li–SO<sub>2</sub> battery was demonstrated for the first time. The electrochemical formation and decomposition of Li<sub>2</sub>S<sub>2</sub>O<sub>4</sub>, the major discharge product of a Li–SO<sub>2</sub> battery, was reversibly possible with a remarkably small charging polarization even without a catalyst. With the aid of a LiI redox mediator, it could exhibit a polarization lower than 0.3 V with one of the highest energy efficiencies achieved for Li–gas battery systems to date. The rechargeable Li–SO<sub>2</sub> battery could deliver approximately 5400 mAh g<sup>−1</sup> at 3.1 V, which is slightly higher than that of the Li–O<sub>2</sub> battery. However, at this stage, the level of cycle performance is limited because of the formation of byproducts, which gradually deposit on the cathode and hinder the efficient cycling. Although a step forward has been made for the secondary Li–SO<sub>2</sub> battery system, issues such as suppression of the byproducts to enhance the cyclability and the identification of an electrolyte capable of dissolving a large amount of SO<sub>2</sub> gas to minimize the emission remain to be resolved. This report may provide an interesting new direction for designing rechargeable battery systems by applying a conventional primary battery chemistry to a viable secondary battery system.

## Experimental Section

**Preparation of Li–SO<sub>2</sub> cells:** The cathode was prepared from a mixture of Ketjen black (KB) and Kynar 2801 as a binder at a ratio of 8:2. The mixture was pasted onto a Ni-mesh current collector. The individual cells were assembled in the sequence of Li metal (3/8 inch diameter), glass fiber separator (Whatman GF/D microfiber filter paper, 2.7 μm pore size), and prepared KB electrode in a Swagelok-type cell. The cathode was open to sulfur dioxide gas. Before the test, all the cells were stabilized for 30 min. The electrolyte

consisted of 1M lithium bis(trifluoromethylsulfonyle)imide (LiTFSI) in tetraethylene glycol dimethylether (TEGDME). In the catalyst-loaded electrolyte, 0.05M LiI was added to the solvent.

Electrochemical characterization and analyses: The electrochemical performances of Li-SO<sub>2</sub> cells were investigated using a potentiogalvanostat (WonA Tech, WBCS 3000, Korea). For the electrode characterization, X-ray diffractometry (XRD, Rigaku, D/MAX-RB diffractometer, Tokyo, Japan), X-ray photoelectron spectroscopy (XPS, Thermo VG Scientific, Sigma Probe, UK), and field-emission scanning electron microscopy (FE-SEM, Philips, XL 30 FEG, Eindhoven, Netherlands) were used. To measure the gas evolution in situ, differential electrochemical mass spectroscopy (DEMS) was used. The DEMS system consisted of a mass spectrometer (MS; HPR-20, Hiden Analytical) and a potentiogalvanostat (WonA Tech, WBCS 3000, Korea), as described in previous reports.<sup>[37,38]</sup> After the discharge process, the cell was transferred to the DEMS cell. Then, the DEMS cell was fully relaxed for 12 h with argon gas flowing (10 ccmin<sup>-1</sup>). The evolved gases were swept by argon gas to the MS chamber during the charge process.

**Keywords:** catalysts · electrochemistry · Li-SO<sub>2</sub> battery · rechargeability · sulfur dioxide

**How to cite:** *Angew. Chem. Int. Ed.* **2015**, *54*, 9663–9667  
*Angew. Chem.* **2015**, *127*, 9799–9803

- [1] K. M. Abraham, Z. Jiang, *J. Electrochem. Soc.* **1996**, *143*, 1–5.
- [2] P. G. Bruce, S. A. Freunberger, L. J. Hardwick, J.-M. Tarascon, *Nat. Mater.* **2012**, *11*, 19–29.
- [3] A. Débart, A. J. Paterson, J. Bao, P. G. Bruce, *Angew. Chem. Int. Ed.* **2008**, *47*, 4521–4524; *Angew. Chem.* **2008**, *120*, 4597–4600.
- [4] H.-D. Lim, H. Song, J. Kim, H. Gwon, Y. Bae, K.-Y. Park, J. Hong, H. Kim, T. Kim, Y. H. Kim, X. Lepró, R. Ovalle-Robles, R. H. Baughman, K. Kang, *Angew. Chem. Int. Ed.* **2014**, *53*, 3926–3931; *Angew. Chem.* **2014**, *126*, 4007–4012.
- [5] Z. Peng, S. A. Freunberger, Y. Chen, P. G. Bruce, *Science* **2012**, *337*, 563–566.
- [6] R. Mori, *RSC Adv.* **2014**, *4*, 1982–1987.
- [7] X. Ren, Y. Wu, *J. Am. Chem. Soc.* **2013**, *135*, 2923–2926.
- [8] P. Hartmann, C. L. Bender, M. Vračar, A. K. Dürr, A. Garsuch, J. Janek, P. Adelhelm, *Nat. Mater.* **2013**, *12*, 228–232.
- [9] S. R. Gowda, A. Brunet, G. M. Wallraff, B. D. McCloskey, *J. Phys. Chem. Lett.* **2013**, *4*, 276–279.
- [10] K. Takechi, T. Shiga, T. Asaoka, *Chem. Commun.* **2011**, *47*, 3463–3465.
- [11] T. Shiga, Y. Hase, Y. Kato, M. Inoue, K. Takechi, *Chem. Commun.* **2013**, *49*, 9152–9154.
- [12] Y. Liu, R. Wang, Y. Lyu, H. Li, L. Chen, *Energy Environ. Sci.* **2014**, *7*, 677–681.
- [13] W. F. Meyers, B. Bell, J. W. Simmons, U.S. Patent 3 423 242, **1969**.
- [14] G. T. K. Fey, *J. Power Sources* **1991**, *35*, 153–162.
- [15] R. L. Ake, D. M. Oglesby, W. P. Kilroy, *J. Electrochem. Soc.* **1984**, *131*, 968–974.
- [16] H. Xing, C. Liao, Q. Yang, G. M. Veith, B. Guo, X.-G. Sun, Q. Ren, Y.-S. Hu, S. Dai, *Angew. Chem. Int. Ed.* **2014**, *53*, 2099–2103; *Angew. Chem.* **2014**, *126*, 2131–2135.
- [17] M. W. Rupich, L. Pitts, K. M. Abraham, *J. Electrochem. Soc.* **1982**, *129*, 1857–1861.
- [18] B. V. Ratnakumar, M. C. Smart, R. C. Ewell, L. D. Whitcanack, A. Kindler, S. R. Narayanan, S. Surampudi, *J. Electrochem. Soc.* **2007**, *154*, A715–A724.
- [19] D. Linden, B. McDonald, *J. Power Sources* **1980**, *5*, 35–55.
- [20] M. M. Ottakam Thotiyil, S. A. Freunberger, Z. Peng, P. G. Bruce, *J. Am. Chem. Soc.* **2012**, *135*, 494–500.
- [21] R. A. Huggins, *Advanced batteries: materials science aspects*, Springer Science, New York, **2008**, pp. 159–195.
- [22] D. W. Ernst, *J. Electrochem. Soc.* **1982**, *129*, 565–567.
- [23] D. Zhai, H.-H. Wang, K. C. Lau, J. Gao, P. C. Redfern, F. Kang, B. Li, E. Indacochea, U. Das, H.-H. Sun, H.-J. Sun, K. Amine, L. A. Curtiss, *J. Phys. Chem. Lett.* **2014**, *5*, 2705–2710.
- [24] D. Oh, J. Qi, Y.-C. Lu, Y. Zhang, Y. Shao-Horn, A. M. Belcher, *Nat. Commun.* **2013**, *4*, 2756.
- [25] J. Hassoun, H.-G. Jung, D.-J. Lee, J.-B. Park, K. Amine, Y.-K. Sun, B. Scrosati, *Nano Lett.* **2012**, *12*, 5775–5779.
- [26] C. Shang, S. Dong, P. Hu, J. Guan, D. Xiao, X. Chen, L. Zhang, L. Gu, G. Cui, L. Chen, *Sci. Rep.* **2015**, *5*, 8335.
- [27] S. Ganapathy, B. D. Adams, G. Stenou, M. S. Anastasaki, K. Goubitz, X.-F. Miao, L. F. Nazar, M. Wagemaker, *J. Am. Chem. Soc.* **2014**, *136*, 16335–16344.
- [28] B. D. Adams, C. Radtke, R. Black, M. L. Trudeau, K. Zaghib, L. F. Nazar, *Energy Environ. Sci.* **2013**, *6*, 1772–1778.
- [29] P. Hartmann, C. L. Bender, J. Sann, A. K. Dürr, M. Jansen, J. Janek, P. Adelhelm, *Phys. Chem. Chem. Phys.* **2013**, *15*, 11661–11672.
- [30] L. Johnson, C. Li, Z. Liu, Y. Chen, S. A. Freunberger, P. C. Ashok, B. B. Praveen, K. Dholakia, J.-M. Tarascon, P. G. Bruce, *Nat. Chem.* **2014**, *6*, 1091–1099.
- [31] N. B. Aetukuri, B. D. McCloskey, J. M. García, L. E. Krupp, V. Viswanathan, A. C. Luntz, *Nat. Chem.* **2015**, *7*, 50–56.
- [32] M. Yu, X. Ren, L. Ma, Y. Wu, *Nat. Commun.* **2014**, *5*, 5111.
- [33] S. A. Freunberger, Y. Chen, Z. Peng, J. M. Griffin, L. J. Hardwick, F. Bardé, P. Novák, P. G. Bruce, *J. Am. Chem. Soc.* **2011**, *133*, 8040–8047.
- [34] H.-D. Lim, K.-Y. Park, H. Gwon, J. Hong, H. Kim, K. Kang, *Chem. Commun.* **2012**, *48*, 8374–8376.
- [35] B. W. Compton, *Sulfur Dioxide: Properties, Applications and Hazards*, Nova Science, New York, **2011**.
- [36] P. G. T. Fogg, W. Gerrard, *Solubility of gases in liquids: a critical evaluation of gas/liquid systems in theory and practice*, Wiley, New York, **1991**.
- [37] H.-D. Lim, H. Gwon, H. Kim, S.-W. Kim, T. Yoon, J. W. Choi, S. M. Oh, K. Kang, *Electrochim. Acta* **2013**, *90*, 63–70.
- [38] B. D. Adams, R. Black, C. Radtke, Z. Williams, B. L. Mehdi, N. D. Browning, L. F. Nazar, *ACS Nano* **2014**, *8*, 12483–12493.

Received: May 12, 2015

Published online: July 3, 2015